Size Effect in Metastable Water

Kirill Shmulovich, Lionel Mercury

Size Effect in Metastable Water

K. I. Shmulovich[a] and L. Mercury[b]

[a]*Institute of Experimental Mineralogy, Russian Academy of Sciences, Chernogolovka, Moscow obl., 142432 Russia*
e-mail: KShmulovich@yandex.ru

[b]*Institut des Sciences de la Terre d'Orleans, ISTO, 1A rue de la Ferollerie, 45071, Orleans, Cedex 2, France*
Received April 14, 2013; in final form November 29, 2013

Abstract—We experimentally determined the maximum tension in synthetic fluid inclusions from the difference between the temperatures of homogenization (T_h) and spontaneous vapor nucleation (T_n). At temperatures of 100–200°C, liquid water may exist at negative pressures of up to 100–150 MPa. Owing to an increase in surface tension, the effect is even more significant in salt solutions and occurs at higher temperatures. A decrease in the linear dimension of fluid phase by an order of magnitude and, correspondingly, a three orders of magnitude decrease in volume (which is proportional to R^3) increase the maximum tension by ~25 MPa. Tension in the liquid phase of water–salt systems may be higher than ~200 MPa without cavitation. Metastability of water and salt solutions in small-sized vacuoles generates stresses in the fluid–mineral system resulting in high solubilities of solid phases. An increase in volume due to coalescence of small inclusions or vanishing of metastability results in an abrupt decrease in supersaturation.

DOI: 10.1134/S0869591114030060

INTRODUCTION

In the petrological and geochemical literature, the thermodynamic properties of components of fluid phases are considered on the basis of experimental and thermodynamic data obtained in macroscopic systems, i.e., with volumes of at least several cubic centimeters. The real portions of fluid phases observed as fluid inclusions and intergranular cavities (especially in metamorphic rocks) are micrometer-sized or even smaller and may be beyond the scale of optical observation. Specific methods have been developed for the investigation of the properties of liquid (liquid-like phase) at the nanometer scale, whereas there are no such methods for the transitional range, which is important for the understanding of mineral forming processes. This paper reports the results of measurements of the parameters of two types of phase transition depending on the size of fluid phase. One type is the ordinary homogenization of a two-phase medium (liquid + vapor), L + V → L. Using the known equation of state of the given liquid, density and pressure can be calculated from the homogenization temperature (T_h). The second type is L → L + V, i.e., the nucleation of a vapor phase in a homogeneous liquid owing to a temperature decrease; it is less popular because of metastability. Under natural conditions, such processes correspond to fluid release during cooling and decompression of magmatic melts and retrograde *P-T* evolution of metamorphic fluid. In addition, this paper considers some physicochemical and mechanical phenomena accompanying a temperature decrease at a microscopic scale. The model of large-scale anatexis is beyond the scope of this study.

PROBLEM FORMULATION

Supersaturation is required for the occurrence of the above phase transitions, because the formation of a nucleus exceeding a critical size is needed for the growth of a new phase, and the fluid must be in a metastable state. The properties of metastable liquids have been extensively investigated, but petrological and geochemical aspects are usually outside the scope of studies in the physics of liquids.

Our study employed the method of synthetic fluid inclusions (SFI) filled with pure water, slightly alkaline solutions, or aqueous salt solutions, which were used as a proxy for the intergranular metamorphic fluid. The obtained results were published by Zheng et al. (1991) and Shmulovich et al. (2009), and there are general reviews on metastable liquids (e.g., Caupin et al., 2012) which paid special attention to stretching, i.e., the state of water and aqueous solutions at negative pressures. Phase diagrams for the *P* < 0 region were presented in textbooks on fluid inclusions (Roedder, 1984); however, they were not calibrated, and their isochors and spinodal are based on the extrapolation of equations of states into the metastable region, in which the *P-V-T* properties of aqueous solutions were never experimentally determined. Moreover, it was supposed that the slope of isochors in a *P–T* diagram changes sharply at zero pressure, i.e., at a change from liquid compression to liquid tension; however, no physical explanation was given for such an inflection.

Based on the theory of homogeneous nucleation, Skripov (1989) concluded that the delay time of the formation of a vapor nucleus with a critical size in a unit volume is a characteristic parameter of the given

liquid and temperature, and, consequently, the delay time of nucleation is inversely proportional to the volume of the system. The radius of a critical nucleus (R_c) depends on two parameters, surface tension on the phase boundary (σ) and pressure in the system (P). These quantities are linked by the Laplace equation:

$$P = 2\sigma/R_c. \qquad (1)$$

As long as vesicles with radii below R_c are formed in a liquid with the given σ value owing to fluctuations, their internal pressure will be higher than P_c, and they will collapse because of the small curvature radius. Pressure lower than P_c will be reached in a nucleus with $R > R_c$; such a vapor bubble will grow, and the metastable liquid will be transformed into a stable state under P and T conditions corresponding to the L + V equilibrium.

Fall et al. (2009) estimated the size effect for quartz-hosted fluid inclusions of pure water with densities corresponding to homogenization temperatures of $T_h < 230°C$. For inclusions ranging in size from a few to tens of micrometers, homogenization temperature increased by 1–3°C with increasing size, and the largest inclusions yielded T_h-based density values most closely corresponding the P-T conditions of synthesis. The authors proposed a simple explanation: the volume proportions of the vapor and liquid phases in small and large inclusions are identical, but during heating the R_c value is reached at lower temperatures in small inclusions. This phenomenon is not related to metastability, because, in a heating cycle, the system occurs in the stable state of the L + V phase equilibrium. In large-scale natural water reservoirs (geyser systems), the overheating above the equilibrium temperature is no higher than ~1°C (Merzhanov et al., 1974). These data indicate that the contribution of the fluid size factor to the uncertainty of estimates of mineral forming parameters at the prograde metamorphic stage (at a temperature increase) is small and can be ignored.

The situation changes fundamentally for the retrograde metamorphic stage. Consider the evolution of a microscopic volume of fluid during cooling. A temperature decrease results in the expansion of immiscibility fields in multicomponent H_2O–CO_2–salt systems (Shmulovich and Graham, 2004) and phase transitions of the L → L + V and L → L + S types in one- and two-component systems (water and salt solution). If the initial composition is close to a phase boundary in the respective T–X diagram, and the fluid occurs in the immiscibility region at the new temperature, the formation of a nucleus of a new phase with $R > R_c$ requires supercooling in the system for the accumulation of energy necessary for the formation of a growing nucleus of the new phase.

In a recent review, Caupin et al. (2012) noted that there are two groups of data on the maximum tension at which spontaneous vapor nucleation occurs in water. The first group includes measurements by the methods of acoustic cavitation, Bourdon tubes, and shockwave experiments. In general, the results obtained by these techniques are well consistent, and only the most comprehensive data of acoustic cavitation are shown in Fig. 1 for the sake of simplicity. These measurements (denoted as AC) plot in the P–T diagram along a curve between −25 MPa near 0°C and −15 MPa at 75°C; at increasing temperature, this curve must terminate at the critical point of water (374°C), but no measurements were made under these conditions.

The second group of data on nucleation pressure comes from the investigation of fluid inclusions (both natural and synthetic). Roedder (1967) described a pure water inclusion without a vapor bubble with a melting temperature of +6.5°C; pressure at the melting point can be estimated for this inclusion as −90 MPa by extrapolating the equilibrium ice melting curve (line S−L in Fig. 1). This was the first evidence for the existence of such tensile stresses in water. The studies of Angell's group (Zheng et al., 1991; Green et al., 1990) revealed nucleation pressures up to −100 MPa and even one inclusion with an estimate of −140 MPa. More detailed measurements were performed by Shmulovich et al. (2009) using the SFI technique. They measured T_h and T_n in samples with SFI containing pure water, alkali solutions (0.1–0.5 m NaOH), and salt solutions (NaCl, CaCl₂, and CsCl) with concentrations of up to 5 m. Within any of these samples, inclusions showed similar T_h values; i.e., the density of liquid was constant in any sample. The measured T_h values define liquid density (i.e., isochore), and T_n is an indicator of the pressure of vapor bubble nucleation. Points corresponding to the nucleation pressures of two samples with pure water isochores of 0.935 and 0.925 g/cm³ are shown in Fig. 1.

In all the aforementioned studies, nucleation pressure was calculated using the IAPWS equation of state of water (Wagner and Pruss, 2002) or the empirical equations of state of Mao and Duan (2008) for water–salt systems. Neither of these equations of state was calibrated at $P < 0$, and pressure estimation was based on the extrapolation of isochores, but this extrapolation is not as straightforward as in the case of the ice melting line. The isochores of water are curved and, moreover, must pass through a minimum at the intersection with the maximum density line (MDL) in Fig. 1. Recently, we measured the difference between the frequency of symmetric stretching vibrations in the Raman spectra of aqueous Na₂WO₄ solutions in a single inclusion at the same temperatures (170–220°C) but in different phase states: equilibrium heterogeneous (L + V) and metastable homogeneous (L only). The result supported the plausibility of isochore extrapolation into the metastable region. Interpolation between pressure measurements by acoustic cavitation at temperatures of 0–75°C and the critical point of water yielded a pressure of approximately −5 MPa at 170°C, and a value of −50 MPa was obtained by
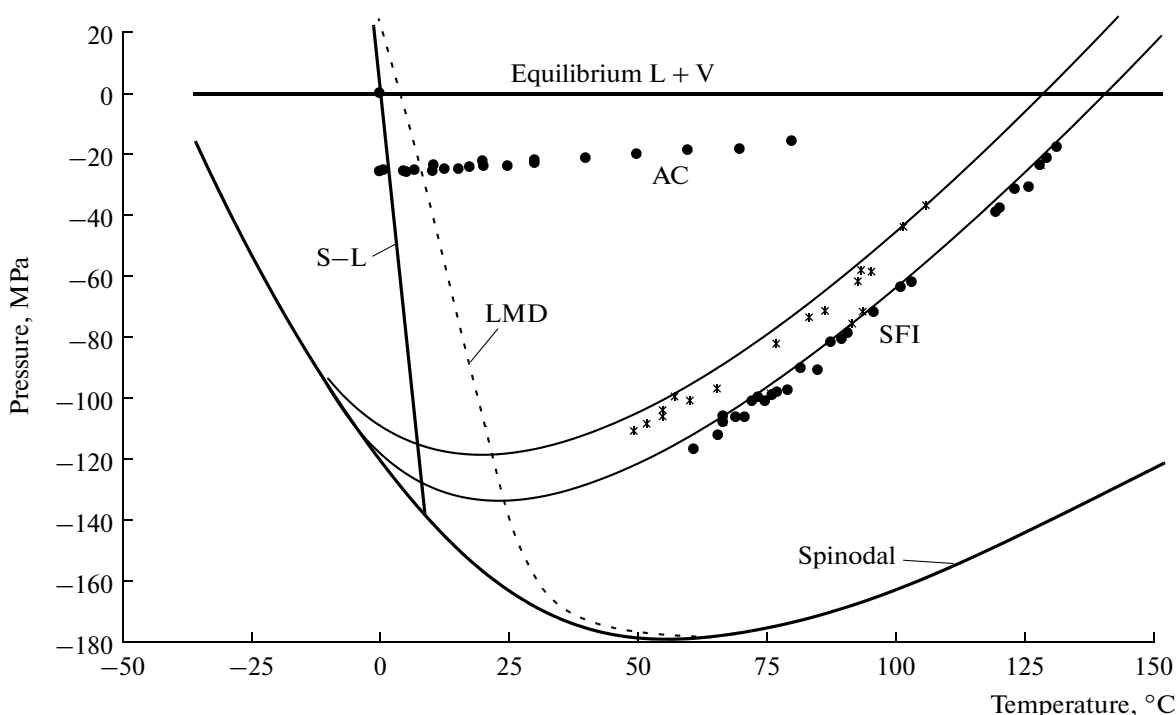
Fig. 1. Simplified fragment of the phase diagram of water in the metastable region, i.e., at negative pressures. AC is the pressure of vapor phase nucleation in acoustic cavitation experiments. SFI refers to the method of measurement of synthetic fluid inclusions and two isochores of 0.935 and 0.925 g/cm^3. LMD is the line of the maximum density of water. S−L is the equilibrium ice melting line. Spinodal is the boundary of the mechanical stability of the system defined from the equation of state under the condition $(\delta V/\delta P)_T = 0$.

direct measurements in SFI using a calibration independent of the equation of state.

A question arises as to the reason for the discrepancy (Fig. 1) between the estimates of the pressure of vapor phase nucleation (synonymous with cavitation) in the same material obtained by the fluid inclusion and other methods. The only fundamental difference between the samples was the volume of the liquid phase. The measured SFI are 5−150 μm in size, whereas the volumes of samples used in experiments on acoustic cavitation, Bourdon tubes, and shockwaves measure in cubic centimeters.

In the standard theory of homogeneous nucleation (THN; Skripov, 1989), the delay time of a phase transition is a reciprocal function of the system volume:

$$\log t \text{ (s)} = A - k_1 \log V \, (\mu m^3). \qquad (2)$$

El Mekki et al. (2010) and subsequently El Mekki (unpublished PhD thesis) measured T_h and T_n and cooled the same inclusions after homogenization terminating the temperature decrease 1−6°C above T_n. They estimated the delay time of nucleation as the mean of 4−5 measurements at such temperatures; i.e., the kinetics of the phase transition into a stable state was explored at tensions approaching the maximum value. It was found that the delay time (t) increases

exponentially (differently for different inclusions) with increasing $T - T_n$:

$$\log t = B + k_2(T - T_n). \qquad (3)$$

Long extrapolation from the delay time of vapor phase nucleation in a water inclusion measured in the laboratory to geologic time scales indicates that even half of the difference $T_h - T_n = 54°C$ (measured in a particular inclusion) is sufficient to provide a delay time of approximately 10 Myr. In Eq. (3), the T value lies within the metastable region, $T_h > T > T_n$. Let us replace variable T in Eq. (3) with T_h (i.e., fix liquid density in the given inclusion) and equate the right-hand sides of Eqs. (2) and (3) at a certain t. After manipulations with constants, we obtain

$$\log V = C + k_3(T_h - T_n). \qquad (4)$$

The T_h value shows only a weak dependence on V (Fall et al., 2009): the difference between large and small SFI is no higher than 1.5−2°C (for SFI with sizes similar to those in our samples). Variations in nucleation temperature (T_n) in a single sample are much greater (by 1−2 orders of magnitude or even more). Hence, the dependence of Eq. (4) is controlled by T_n.

One of the goals of this paper was the determination of the C and k_3 coefficients of Eq. (4). However, two comments should be made before discussing the measurements.
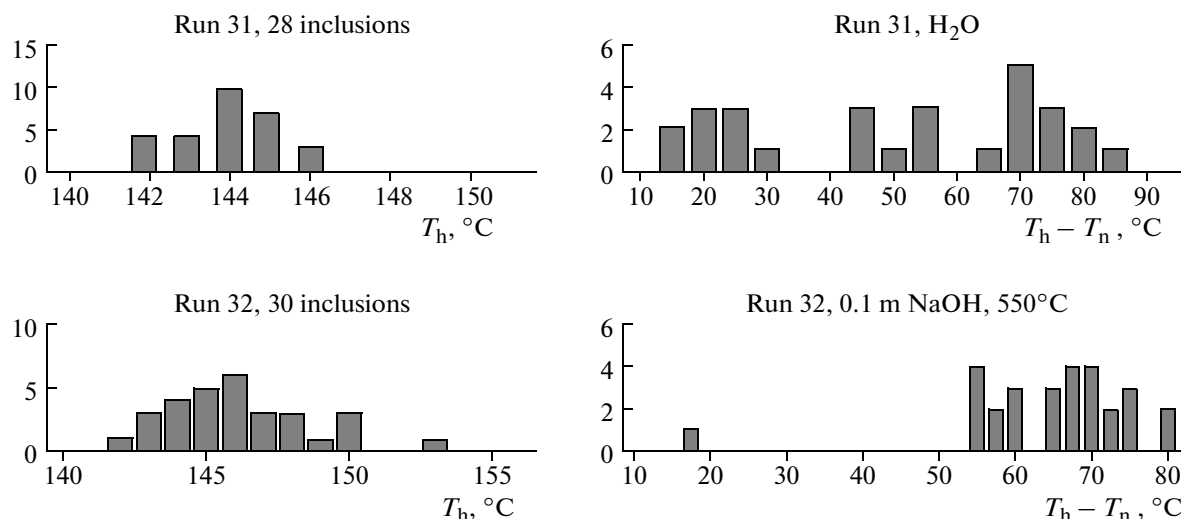
Fig. 2. Histograms of the temperatures of homogenization (T_h) and vapor phase nucleation (T_n) in samples of two parallel experiments on the formation of SFI at 550°C and ~700 MPa. Inclusions in the sample of experiment 31 contained pure water ($T_h = 143.5 \pm 1$°C), and those from experiment 32 contained 0.1 m NaOH solution ($T_h = 145.9 \pm 2.5$°C). The sample of experiment 32 is almost free of inclusions with relatively high temperatures of vapor phase nucleation, i.e., $T_h - T_n < 50$°C, whereas such inclusions account for almost half of the inclusion population of experiment 31.

It can be seen in Fig. 1 that T_n of SFI with pure water from a single sample varies considerably at a constant density (T_h variations are within ±2°C), and the difference $T_h - T_n$ ranges from 15 to 80°C. Such considerable variations in T_n are related mainly to heterogeneous nucleation; i.e., roughnesses and fissures on the inner surface of the crystal (in general, singularities) induce early (compared with that predicted by THN) vapor phase nucleation. According to THN, the formation of a growing vapor nucleus results from random fluctuations in liquid density and is inherently probabilistic. The probability of a fluctuation causing the formation of a growing nucleus increases with increasing stretching of the liquid (remoteness from the equilibrium state in more general terms), which is necessary to rupture the continuity of condensed matter. Heterogeneous nucleation is also probabilistic, but singularities on the inclusion surface reduce the activation barrier, and cavitation occurs at lower tensions compared with homogeneous nucleation. Shmulovich et al. (2009) showed that T_n variations can be significantly decreased if pure water is replaced in SFI with a medium that more efficiently dissolves the host mineral. Figure 2 shows the histograms of T_h and $T_h - T_n$ measured in two samples with pure water (run 31) and 0.1 m NaOH solution (run 32) synthesized under identical conditions. Approximately 30 inclusions were measured in each of the samples. The T_h values showed only minor differences, but inclusions with $T_h - T_n < 55$°C were very rare in the sample of run 32 and accounted for half of the inclusion population of run 31. In other experiments, 0.2 and 0.5 m NaOH solutions were used, but the scatter of $T_h - T_n$ in these experiments was almost identical to that observed in

the case of 0.1 m solution (run 32). The reduction of the scatter owing to the disappearance of inclusions with relatively high T_n implies extensive removal of singularities from the inclusion surface; however, they probably cannot be completely eliminated in synthetic samples. In order to minimize the effect of heterogeneous nucleation in the experiments described below, the duration of synthesis at similar temperatures was increased threefold compared with runs 31 and 32.

Besides dependence (4), another factor is the possible nonisochoric behavior of SFI at tensions approaching the maximum values. If tensile stress reaches ~100 MPa or more during cooling, elastic deformations may slightly change the inclusion volume. The nonisochoric behavior of large (50–100 μm) and especially flattened inclusions with pure water at the maximum tensions was demonstrated on the basis of sound velocity data (Alvarega et al., 1992); therefore, such inclusions were not used for measurements. The inclusions that were selected for measurements were usually isometric in plan view and showed developed or incipient equilibrium patterns, i.e., faces and edges of a negative crystal.

EXPERIMENTAL METHODS

In order to quantify the size effect, fluid inclusions with 0.1 and 0.2 m NaOH solutions were synthesized at the Institute of Experimental Mineralogy, Russian Academy of Sciences. Inclusions in quartz were produced by the method of Bodnar and Sterner (1985) using an internally heated pressure vessel at 600 MPa, 500°C, and a run duration of 30 days. Quartz prisms 3 × 3 mm across and 15 mm long (along the *c* axis)

were rinsed in hot diluted HF and loaded into Pt capsules ($4 \times 40 \times 0.2$ mm) with ~10 mg of amorphous silica. After adding approximately 100 μL of solution, the capsule was welded shut and checked for leaks by heating in an oven at 120°C overnight. After treatment under the desired P-T conditions, the capsule was checked for weight gain or loss, which should be within ±0.2 mg. The prisms were sectioned into 0.7 mm thick wafers across the c axis, ground on either side with silicon carbide paper, polished with wet CeO, and washed in acetone in an ultrasonic bath.

A Linkam TS-600 heating/freezing stage was used to measure the sizes of inclusions, homogenization temperatures upon heating (T_h), and temperatures of spontaneous nucleation of a vapor bubble upon continuous cooling (T_n) at rates of 5 and 2°C per minute.

MEASUREMENTS AND OBSERVATIONS

Similar to our previous study (Shmulovich et al., 2009), we measured the temperatures of the $L + V \rightarrow L$ phase transition upon heating (homogenization to a liquid, T_h) and the reverse transition $L \rightarrow L + V$ (i.e., nucleation of a vapor phase) upon cooling (T_n). During SFI heating, the volume of a gas (vapor) bubble decreases gradually owing to the thermal expansion of liquid phase, and pressure increases along the $L + V$ equilibrium curve. Usually, the measurement of T_h in undersaturated solutions ($L + V$) does not present problems: when the gas bubble becomes smaller than the optical resolution, its chaotically moving shadow becomes clearly visible. A few inclusions in which T_h could not be determined, because their gas bubbles escaped into an opaque zone, were not used for statistical analysis. The scatter of measured T_h values was due to temperature gradients during measurements, both in the Linkam stage and along the quartz prism that was used as a seed during synthesis.

In contrast to T_h, the measurement of T_n is more problematic. The phenomenon of unmixing (cavitation) is easily observed, especially at the hysteresis $T_h - T_n > 20°C$. At a small hysteresis, the absence of real homogenization is possible, and the gas bubble grows gradually in such a case. After complete homogenization, cavitation (i.e., phase transition) occurs at tension, which results in the instantaneous formation of a clearly visible gas bubble. Occasionally, 2−3 bubbles appear simultaneously. A video clip showing intense retrograde boiling in an inclusion with 5 m NaCl solution is available at http://www.iem.ac.ru/staff/kiril/.

The reproducibility of T_h and T_n values was estimated previously for a sample with 5 m NaCl solution at heating/cooling rates of 1−5°C/min. Under such conditions, the scatter of measured values was no higher than 0.2°C for both T_h and T_n. The change of T_n depending on cooling rate in the measurements reported by El Mekki-Azouzi et al. (2012) was most

likely related to a temperature gradient between the inclusion and the silver block of the Linkam stage; i.e., this is an artifact. These authors measured nucleation in one inclusion from a sample synthesized in an internally heated pressure vessel (run 37) at 530°C, 750 MPa, and a duration of 9 days ($T_h = 134.7°C$ and $d = 0.923$ g/cm^3). The samples of this series ($2 \times 2 \times 0.5−0.7$ mm in size) were polished manually, and their edges were usually rounded, which resulted in a poor contact between the sample and a sapphire disk placed on the silver block of the Linkam stage and slow heat transfer from the disk to the sample.

The size of SFI was determined using a calibrated ocular micrometer and appropriate objective lenses (×20 and ×40). The available optical equipment did not allow us to employ modern software for more accurate size measurement; therefore, inclusions were selected with nearly cylindrical shapes, diameters of no less than 5−7 μm, and aspect ratios of $l : s > 2$. Figure 3 shows the histograms of T_h and $T_h - T_n$ values, as well as the dependence of $T_h - T_n$ on $\log V$ (μm^3). The results of previous experiments (Shmulovich et al., 2009) recalculated similar to runs 171−175 are also plotted in Fig. 3.

The scatter of T_h values in runs 172 and 175 is +2°C around the most frequent value of 174°C, whereas all the measurements for run 171 fall within 176−179°C without a distinct maximum. Variations in T_h within a single sample are related to two main reasons: temperature gradient in the pressure vessel during fluid inclusion synthesis and temperature gradient within the sample during T_h measurement, which was somewhat higher than the ordinary value, because the quartz wafer was 0.5−0.6 mm thick after polishing.

The reasons for the T_n and, correspondingly, $T_h - T_n$ variations are more complex. Temperature gradient in the gas pressure vessel is of minor significance, because an increase in T_h results in a decrease in SFI density and, consequently, and increase in T_n. The maximum tension values may be affected by sample thickness, because SFI occurring near the upper surface of the wafer may have T_h several degrees higher in a heating cycle and T_n lower in a cooling cycle compared with the respective values for SFI occurring at the bottom of the sample near the silver block of the Linkam stage. All our experiments were performed at cooling/heating rates of 2−5°C/min. Finally, the dependence under question (Eq. 4) is accompanied by uncertainty related to heterogeneous nucleation on singularities on the inclusion walls. In order to diminish the contribution of this phenomenon, alkaline solutions were used (see note to Fig. 2), and the duration of synthesis was increased to one month.

In addition to the errors of measurement of T_n and, as a consequence, $T_h - T_n$, the scatter of hysteresis values has an obvious physical nature. At temperatures close to T_n, the liquid undergoes a strong tensile stress, and any random density fluctuation with $R > R_c$ causes
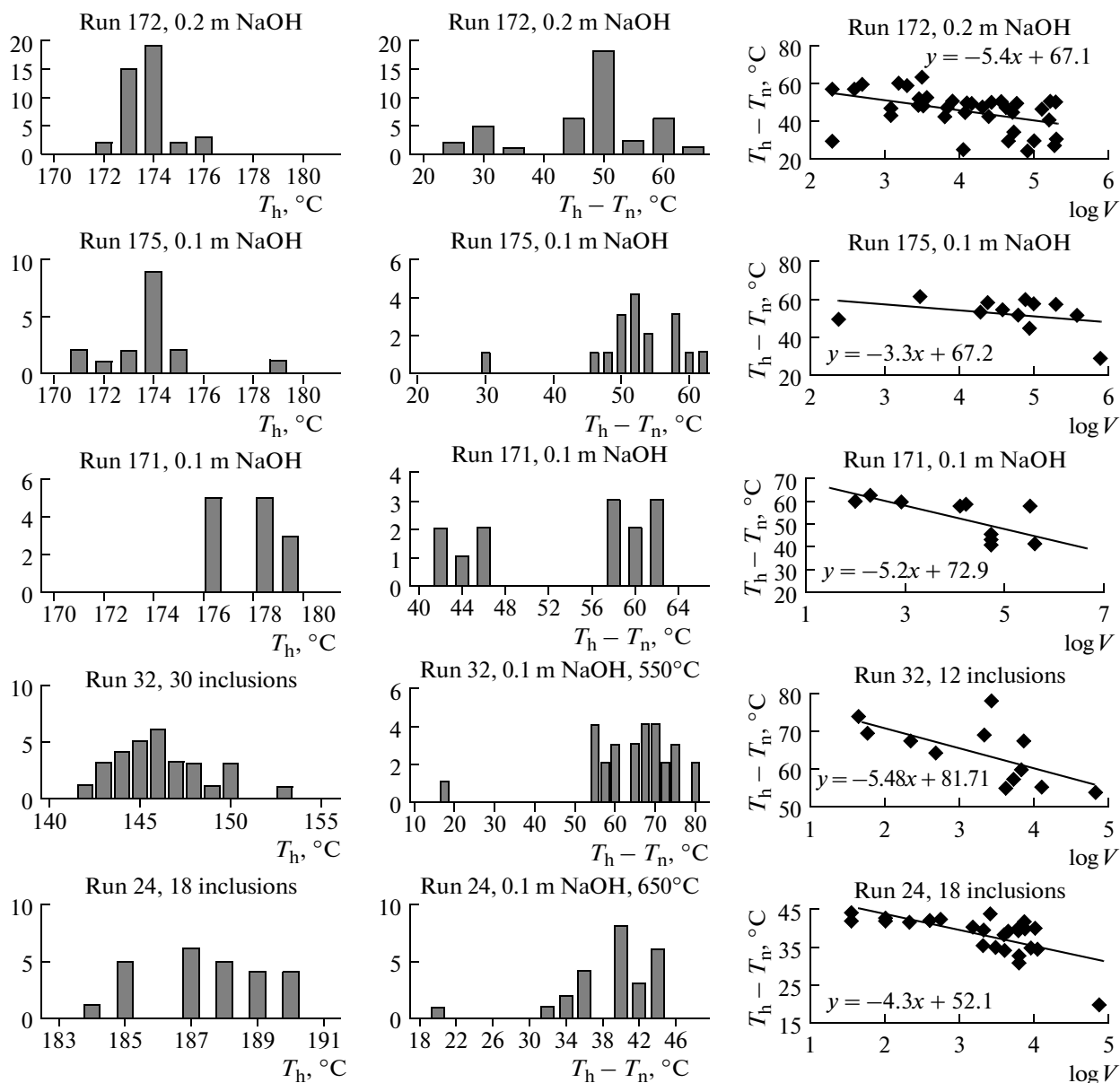
Fig. 3. Histograms of homogenization temperatures (T_h) and hysteresis values ($T_h - T_n$) for samples from experiments 171, 172, and 175 performed under identical parameters. The right column shows the dependence of hysteresis on $\log V$ (μm^3). Experiment 24 was carried out with 0.1 m NaOH solution at 750 MPa and 650°C, experiment 34 was carried out with pure water at 750 MPa and 700°C, and experiment 5 was carried out with 5 m CsCl solution at 650°C and 750 MPa.

the formation of a growing gas bubble and transition of the system into a stable state. The kinetics and activation energy of this process were discussed by El Mekki-Azusi et al. (2014). Here we note only that the delay time of vapor nucleation increases with a probability of 0.5 by two orders of magnitude (per second) for every 4°C "undercooling" relative to T_n. For instance, in a pure water inclusion with $T_h = 144$°C, $T_n = 89$°C, and $T_h - T_n = 55$°C, the measured delay time of nucleation is more than 10 h, if cooling is terminated at $T = 94$°C (measured using four video records). The extrapolation of the observed depen-

dence of nucleation delay time on $T - T_n$ within the range $1-5$°C (almost linear in $\log t$, s) suggests that the nucleation delay time (i.e., the lifetime of the metastable state) will be ~10 Myr at the middle of the above $T_h - T_n$ interval ($T - T_n = 27$°C).

The theory of homogeneous nucleation considers the formation of a growing vapor nucleus as a result of random fluctuations in liquid density. This process can be triggered by heterogeneous nucleation on a phase boundary (inclusion walls), because the limited time of experiment allows the formation of singularities on

this surface. This is the reason for significant T_n variations at a rather narrow T_h range (3–5°C).

The choice of alkaline solutions instead of pure water is based on previous observations. At identical synthesis conditions, SFI with such solutions show a much lower T_n scatter compared with pure water inclusions. This is related to two effect related to the elevated solubility of quartz in alkaline solutions: (a) the number of singularities inducing early heterogeneous nucleation on the inclusion surface is reduced, and (b) the number of flattened inclusions, the isochoric nature of which is not preserved during cooling, is also decreased (Alvarega et al., 1992). According to Brillouin spectroscopy, the volume and sound velocity in large and flattened inclusions are not constant at significant stretching related to the $T_h - T_n$ hysteresis. Other properties of liquids that are important for our study (density and surface tension) are almost identical in water and alkaline solutions. In some sense, the use of alkaline solution allowed us to diminish the period of formation of high-quality inclusions with a small number of singularities on the walls from natural to laboratory time-scales.

The size effect is illustrated by the third column of Fig. 3. The maximum number of inclusions (42) were measured in a sample from run 172 with an NaOH concentration twice as high as that in runs 171 (12 inclusions) and 175 (20 inclusions).

In two of the three samples, the slope of $T_h - T_n$ dependence on volume is slightly higher than 5°C per one logarithmic unit of volume in cubic micrometers, whereas a slope of 3.3°C was obtained for sample 175. It should be noted that no inclusions were rejected from the dataset used for the construction of histograms and regression analysis, and the only selection criterion was the possibility of T_h and T_n measurement. Inclusions were rejected if their T_h values were nonreproducible (decrepitated during heating) or the vapor bubble escaped into a shadow zone near a face or another inclusion below T_h.

Figure 3 shows also the data on inclusions from experiments 24, 34, and 5 (Shmulovich et al., 2009), the sizes of which were measured but not discussed previously. Experiment 24 was carried out using the same 0.1 m NaOH solution (24 inclusions) as runs 171 and 175, but at 0.75 GPa and 650°C. As can be seen in Fig. 3, the slope of $T_h - T_n$ versus $\log V$ (4.3°C per one log unit of V) for a sample from experiment 24 is similar to those from experiments 171, 172, and 175. The sample of run 34 contains pure water inclusions (32 inclusions were measured) synthesized at 0.75 GPa and 700°C. Pure water inclusions usually show a wide scatter in T_n because of the poor quality of the interphase boundary (Fig. 2), but the slope (i.e., k_3 in Eq. (4)) obtained for this sample is similar to that of the sample of run 175, and the intersection with $\log V = 1$ indicates a hysteresis of ~40°C owing to the higher temperature of synthesis.

For comparison, the table includes similar data on 66 two-phase (L + V) undersaturated water–salt inclusions (5 m CsCl solution) from experiment 5 at 0.75 GPa and 600°C. The samples with CsCl solutions showed the maximum hysteresis values (up to 145°C!), but they were not used in this study, because the estimation of the pressure of spontaneous nucleation was hindered by the lack of the equation of state. It should be noted that the concentrated solutions of this salt show a salt-in effect within a wide P-T range, i.e., the solubility of SiO_2 increases with increasing salt concentration, in contrast to NaCl and $CaCl_2$ solutions and H_2O–CO_2 mixtures, which usually show a salt-out effect (Shmulovich et al., 2006). In experiment 173 (parallel with runs 171–175) with a strongly oversaturated CsCl solution (consisting of three phases at 20°C, L + V + S), a statistically significant correlation of $T_h - T_n$ and $\log V$ was also observed, but it was accompanied by as yet poorly understood effect of double metastability, when a stretched liquid becomes oversaturated with respect to the vapor and solid phases. This state is currently under investigation.

Since inclusions with linear dimensions from 5 to 150 μm were measured, the $\log V$ values ranged over four orders of magnitude. This is only a small interval of SFI sizes, but the consistency of results from five independent experiments allows us to use the obtained slope, $k_3 = ~3$–5°C per unit $\log V$, for the estimation of $T_h - T_n$ at smaller sizes. Unfortunately, the available optical instruments offered little opportunity to observed phase transitions in smaller SFI.

In our earlier experiments with aqueous salt solutions (Shmulovich et al., 2009), the length and width of inclusions were measured in the observation plane. Inclusions with NaOH and CsCl solutions showed a negative correlation between $T_h - T_n$ and size, whereas no or a very weak correlation existed for water and NaCl and $CaCl_2$ solutions because of the short experiment duration, which was insufficient to decrease the amount of singularities on the surface of SFI.

DISCUSSION

The slope of the isochore of high-density water ($d > 0.85$ g/cm^3) is weakly dependent on temperature and is ~1.5 MPa/°C up to 150°C near the L + V equilibrium line. Thus, a 3–5°C increase in hysteresis corresponds to a ~5–8 MPa increase in tension per one order of magnitude of a volume decrease. The volumes of macroscopic liquid objects used for the measurement of pressures at acoustic cavitation, by Bourdon tubes, and in shockwave experiments range from a few to tens of milliliters ($N \times 10^{12}$–10^{13} μm^3). Our inclusions measure ~$N \times 10^3$ μm^3; i.e., the difference is 9–10 orders of magnitude. This implies that at a given temperature, the difference in nucleation pressure between the macroscopic samples and SFI will be ~50–80 MPa, which is well consistent with the pressure difference in Fig. 1. In this figure, at identical

Mean homogenization temperatures, densities, and parameters of Eq. (4)

Run no.	T_h, °C	±°C	d, g/cm^3	±	C	k_3
171	178	2	0.8892	0.0021	67.1	5.4
172	174	2	0.8934	0.0021	67.2	3.3
175	174	5	0.8934	0.0051	72.9	5.2
24	188	3	0.8784	0.0033	52.1	4.3
34	205	3	0.8588	0.0036	38.8	3.2
5	170	4			90.2	8.1

Density is unknown in run 5, because there is no equation of state for CsCl solutions.

temperatures of 50−70°C, the difference between the nucleation pressures at acoustic cavitation (AC) and in our inclusions (SFI) is ~80 MPa.

Such a good agreement (within an order of magnitude) between the pressure dependences of the hysteresis ($T_h − T_n$) on the volume of the system obtained from a direct experiment and from a comparison of SFI and acoustic cavitation data allows us to accept the coefficients of Eq. (4), i.e., C and k_3 in the third column of Fig. 3 and the table, as a first approximation. It is important to emphasize that both SFI and samples for acoustic cavitation experiments are obviously macroscopic systems, because a typical inclusion with a size of, say, $10 \times 10 \times 30$ μm contains ~10^{13} water molecules.

The extrapolation of the obtained dependence into the region of inclusion sizes comparable with the wavelength of visible light, a water body of ~1 μm^3 (log $V = 0$) will show a hysteresis value of approximately 70°C, which corresponds to a negative pressure of ~100 MPa. At smaller nanometer-scale linear sizes, metastable states can be expected practically near the theoretical limit (spinodal), where the mechanical stability of the system vanishes (spinodal is a line in a phase diagram, for which $\delta V/\delta P = 0$ according to the equation of state). The spinodal of water−salt systems lies at pressures much lower than that shown in Fig. 1 for water and ends in the critical point of the solution, i.e., at $T > T$(crit) H_2O.

POSSIBLE APPLICATIONS OF THE RESULTS

The main outcome of the experiments reported in this paper is the estimation of the coefficients of Eq. (4), which links SFI volume with the nucleation temperature of vapor phase (T_n) at a given T_h. Almost pure water was used in the experiments; the content of NaOH admixture was no higher than 1−2 molecules per ~550 water molecules, and in fact it was even lower owing to the formation of Na_2SiO_3 solution through an alkali−quartz reaction. In order to apply the obtained data, it is necessary to determine the boundaries of the occurrence of the effects under scrutiny and the tendencies of their changes at a transition to more realistic models of natural fluids.

The technique used to obtain metastable water in SFI is based on the isochoric behavior of isolated liquid portions; consequently, this model can be applied only for the objects in which fluid does not form a system of interconnected pores. This is possible, for instance, at a very low fluid fraction; i.e., when its amount is insufficient to form a three-dimensional network of interconnected channels. Another situation favorable for the formation of isolated water pockets occurs in the P-T interval in which the water phase does not wet the grain boundaries of the silicate matrix. Holness (1992, 1995) measured the wetting of quartz and quartz + feldspar mixtures at 400 MPa and within a wide temperature range. Under such pressure, quartz (quartzite) is not wetted by water fluid at 1100−400°C, and isolated pockets will persist in such rocks up to low-temperature metamorphism. This interval is significantly smaller in a quartz−feldspar matrix (from 400 to ~700°C), but it overlaps the important region of medium-temperature processes. It is interesting that the temperature of a change from nonwetting to wetting behavior during heating of quartz−feldspar rocks almost coincides with the beginning of migmatization (~680°C) at the prograde stage. The physical transition during cooling from wetting to nonwetting behavior implies a change in the fluid state from spreading over the edges and faces of the minerals of the host rock to droplike isolated intergranular pockets and, correspondingly, an increase in the volume/surface (V/S) ratio. An increase in this parameter must enhance the activity (chemical potential) of water without a change in its amount owing to the decrease of interaction of water dipoles with uncompensated charges on the surface of solid phases.

The one-component model (water) can be extended to a more complex multicomponent system
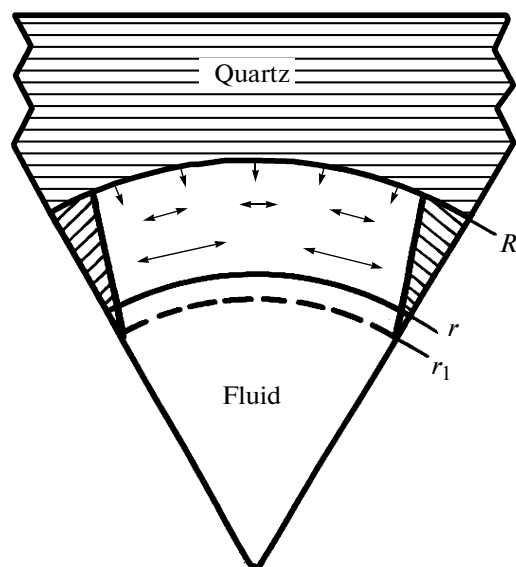
Fig. 4. Scheme of the formation of tangential compression in quartz (double arrows) at negative pressures (tension, single arrows) of fluid in SFI (out of scale). R is the radius of SFI cross-section under equilibrium, r_1 is the radius compensating tension in SFI, and r is the radius of a steady state after the dissolution of strongly compressed layers. The oblique hatching shows a decrease in the circumference requiring compensation.

only hypothetically. The influence of admixtures of nonpolar gases (CO_2 and N_2) on the metastable state of liquid water is unknown, although the metastability of one-component systems of such a kind was measured and was detected even in liquid helium. The first estimates of the influence of salt components were reported by Shmulovich et al. (2009), and here we recall briefly the main results. Inclusions with NaCl, CsCl, and $CaCl_2$ solutions undersaturated under ambient conditions (L + V) with concentrations below 5 m existed in a metastable state within a temperature range ($T_h - T_n$) similar to that characteristic of water inclusions synthesized under the same conditions. The main difference is a shift of T_h and T_n toward higher temperatures. For instance, experiments 63 and 69 were performed in a single autoclave at 300°C and ~200 MPa with 0.2 m NaOH and 4 m NaCl + 0.05 m NaOH solutions, respectively. The inclusions synthesized in these experiments showed T_h values of 177.5°C (run 63) and 188.5°C (run 69). The difference between the $T_h - T_n$ values is relatively small: 50–65°C in run 63 and 60–70°C in run 69.

The results of experiments with higher salinity solutions cannot be easily interpreted because of the appearance of a third phase (salt crystals) in SFI. The homogenization temperature increases at higher salt concentrations, but salt crystals induce early boiling in many inclusions ($T_h - T_n < 25$°C). Three-phase inclu-

sions (S + L + V) with T_h = 250–300°C were obtained in some experiments. Although most of the SFI show small hysteresis values during cooling (<25°C), a few inclusions with $T_h - T_n$ ~ 90–100°C were observed in each sample with NaCl and $CaCl_2$ solutions. Hysteresis values of up to 140°C were observed in inclusions of CsCl solutions consisting of three phases under ambient conditions.

The surface tension (σ) of water decreases almost linearly from 75 mN/m at 0°C to zero at critical temperature (374°C). In samples shown in Fig. 2, the mean vapor nucleation temperature is 120–140°C, and σ ~ 60 mN/m under such conditions. However, the σ value of solution increases linearly with increasing salinity (Fig. 11 in Fall et al., 2009), and anhydrous NaCl melt has a σ of ~100×10^4 N/m at 800–1000°C (*Handbook of...*, 1971). The surface tension of intermediate water–salt compositions can be estimated by interpolation, but this is practicable only for solutions of known salt concentrations. There is no doubt now that concentrated salt solutions approaching the properties of salt melts may exist during metamorphism (Newton et al., 1998).

The results described above revealed the following.

1. The metastable region (hysteresis) expands with decreasing size of isolated fluid vacuoles, and, correspondingly, the maximum tension in water increases and may reach 100–150 MPa.

2. The temperatures of phase transitions (L + V → L and L → L + V) and hysteresis values increase in aqueous salt solutions, and the maximum tension may be as high as 150–200 MPa (estimate from $T_h - T_n$ and a mean water isochore slope of 1.5 MPa/°C).

Another size effect can be predicted from the analysis of geometric relationships for a small-sized isolated fluid phase. Let us consider pressure evolution during the cooling of an initially equilibrium system consisting of water fluid in a quartz matrix. The thermal expansivity coefficients of water and quartz differ by an order of magnitude, and a decrease of pressure in the fluid will outstrip pressure equilibration, because dislocation creep requires a pressure difference as a driving force (Poirier, 1985). Stresses will appear in the crystal, and their tensor will depend on the orientation of the crystal relative to the main compressional vector and the pressure difference. For simplicity, let us consider an isotropic model, in which a water inclusion can be approximated by a sphere or a cylinder. The cross-section of such an inclusion is a circle, a sector of which is schematically shown in Fig. 4. Under equilibrium at $P_{fl} = P_{sol}$, the radius of the circle is R. At $P_{fl} < P_{sol}$, radial stresses toward the center (indicated by single arrows) reduce the inclusion radius to r_1. Tangential stresses develop in the $R - r_1$ layer owing to a decrease in its circumference (double-sided arrows). These stresses are proportional to $R - r_1$, and the degree of compression of the near-surface layers of the matrix is indicated by slanted hatching. As a result,

the $R - r_1$ layer undergoes radial tension and tangential compression. Such a behavior is independent of the absolute value of P_{fl}, which can be both positive and negative, because the condition of the occurrence of the scheme in Fig. 4 is $P_{fl} < P_{sol}$.

The thermodynamics of nonhydrostatically stressed systems was considered by Ostapenko (1977). If the solubility of the host mineral in a fluid is negligible (e.g., in CO_2), the relation $P_{fl} < P_{sol}$ can persist long enough to permit equilibration in decarbonation reaction at unequal P_{fl} and P_{sol} even under laboratory conditions. For a water fluid, the lifetime of a state with $P_{fl} < P_{sol}$ is short, and the system rapidly comes to $P_{fl} = P_{sol}$ at laboratory time-scales. The convergence of P_{fl} and P_{sol} is caused by the dissolution of the matrix material in the regions of high stresses (P_{sol}) and precipitation in the regions of lower pressures. Referring to the scheme shown in Fig. 4, this mechanism will cause the dissolution of the $r - r_1$ layer.

The efficiency of this mechanism can be illustrated by a simple geometrical calculation for the configuration presented in Fig. 4 taking into account the number of molecules in a quartz-hosted cylindrical water (salt solution) inclusion with a diameter of 10 μm. The equilibrium quartz solubility in water at 500°C and 500 MPa is 0.2 mol % and two times lower in 25 mol % NaCl solution (Shmulovich et al., 2006). If the excess chemical potential of SiO_2 induced by tangential stresses will cause the dissolution of a 0.5-nm thick quartz layer, the Si content in each element of the cylindrical vacuole with a diameter of 10 μm will increase by 25% in pure water solution. The Si content will increase by a factor of 3 in a cylinder with a diameter of 1 μm = 1000 nm and by a factor of 25 in a cylinder with a diameter of 100 nm! This results from the fact that the volume of a cylinder is proportional to R^2, while the surface is proportional to R. These estimate will be two times higher, if the initial SiO_2 content will be 0.1 mol % (NaCl solution−melt). Furthermore, if the same process will result in the dissolution of several rather than one surface layer of quartz, the estimates will be several times higher. The properties of such oversaturated solutions (relative to equilibrium at given T and P) may be significantly different from those determined in a large fluid volume, but this problem will be addressed in future studies.

CONCLUSIONS

In agreement with the theory of nucleation (Skripov, 1989), the lower the volume of the fluid phase, the longer the delay time of the phase transition from a metastable to a stable state, or, at a constant time, the higher the tension that liquid water can sustain without cavitation. Owing to an increase in surface tension, the effect will be greater in aqueous salt solutions and must occur at higher temperatures.

A decrease in the linear dimension of fluid phase by one order of magnitude and, correspondingly, a decrease in volume by three orders of magnitude (being proportional to R^3) increases the maximum tension by ~25 MPa in an inclusion with a density of >0.85 g/cm³. The maximum tension for a water volume of ~1 μm can be estimated from the coefficients of Eq. (4) and an isochore slope of 1.5 MPa/°C as 100−150 MPa. In water−salt systems, tensions higher than 200 MPa can exist in a liquid phase without cavitation.

It was predicted that, owing to the difference in the thermal expansivity coefficients of minerals (in particular, quartz) and water (solutions) and the metastable water state in small-sized inclusions, nonhydrostatic stresses are developed in the fluid−mineral system inducing an increase in the solubility of solid phases.

REFERENCES

Alvarega, A.D., Grimsditch, M., and Bodnar, R.J., Elastic properties of water under negative pressures, *J. Chem. Phys.*, 1992, no. 11, pp. 8392−8396.

Bodnar, R.J. and Sterner, S.M., Synthetic fluid inclusions in natural quartz. II. Application to *PVT studies, Geochim. Cosmochim. Acta*, 1985, no. 9, pp. 1855−1859.

Caupin, F., Arvengas, A., Davitt, K., et al., Exploring water and other liquids at negative pressures, *J. Phys. Condens. Matter*, 2012, p. 24.

Fall, A., Rimstidt, J.D., and Bodnar, R., The effect of fluid inclusion size on determination of homogenization temperature and density of liquid-rich aqueous inclusions, *Am. Mineral.*, 2009, vol. 94, pp. 1569−1579.

Green, J.L., Durben, D.J., Wolf, G.H., and Angell, C.A., Water and solutions at negative pressure: Raman spectroscopic study, *Science*, 1990, vol. 249, pp. 649−652.

Holness, M.B., Equilibrium dihedral angles in the system quartz−CO_2−H_2O−NaCl at 800°C and 1−15 kbar: the effect of pressure and fluid composition on the permeability of quartzites, *Earth Planet. Sci. Lett.*, 1992, vol. 114, pp. 171−184.

Holness, M.B., The effect of feldspar on quartz−H_2O−CO_2 dihedral angles at 4 kbar, with consequences for the behaviour of aqueous fluids in migmatites, *Contrib. Mineral. Petrol.*, 1995, vol. 118, pp. 356−364.

Janz, G.J., *Molten Salts Handbook*, New York: Academic Press, 1969.

Mao, S.D. and Duan, Z.H., The *PVTX* properties of binary aqueous chloride solutions up to $T = 573$ K and 100 MPa, *J. Chem. Thermodyn.*, 2008, vol. 40, no. 7, pp. 1045−1063.

El Mekki, M., Ramboz, C., Lenan, J.F., and Shmulovich, K., Kinetic law of stretched water and aqueous solutions in micrometric synthetic fluid inclusions. Part 1—Nucleation rates, *J. Chem. Phys.*, 2014 (in press).

El Mekki-Azouzi, M., Ramboz, C., Lenain, J.F., and Caupin, F., A coherent picture of water at extreme negative pressure, *Nature Physics*, 2012, vol. 2475. DOI: 10.1038, 1−4.

Merzhanov, A.G., Shteinberg, A.S., and Shteinberg, G.S., On the modeling of the geyser process, *Geokhimiya*, 1974, no. 2, pp. 277−290.

Newton, R.C., Aranovich, L.Ya., Hansen, T.C., and Vandenheuvel, B.A., Hypersaline fluids in Precambrian deep-crustal metamorphism, *Precambrian Res.*, 1998, vol. 91, pp. 41−63.

Ostapenko, G.T., *Termodinamika negidrostaticheskikh sistem i ee primenenie v teorii metamorfizma* (Thermodynamics of Nonhydrostatic Systems and Its Application to the Theory of Metamorphism), Kiev: Naukova dumka, 1977.

Poirier, J.P., *Creep of Crystals*, Cambridge−New York−Melbourne: Cambridge Univ., 1985.

Roedder, E., *Fluid Inclusions in Minerals. Rev. Mineral.*, 1984, vol. 12.

Shmulovich, K.I. and Graham, C., An experimental study of phase equilibria in the systems $H_2O-CO_2-CaCl_2$ and H_2O-CO_2-NaCl at high pressures and temperatures (500−800°C, 0.5−0.9 GPa): geological and geophysical applications, *Contrib. Mineral. Petrol.*, 2004, vol. 146, pp. 450−462.

Shmulovich, K.I., Yardley, B.W.D., and Graham, C., The solubility of quartz in crustal fluids: experiments in salt solutions and H_2O-CO_2 mixtures at 400−800°C and 0.1−0.9 GPa, *Geofluids*, 2006, vol. 6, pp. 154−167.

Shmulovich, K.I., Mercury, L., Thiery, R., et al., Experimental superheating of water and aqueous solutions, *Geochim. Cosmochim. Acta*, 2009, vol. 73, pp. 2457−2470.

Skripov, V.P., Metastable phases as relaxing systems, in *Termodinamika metastabil'nykh sistem* (Thermodynamics of Metastable Systems), Sverdlovsk: Ural. Otd. AN SSSR, 1989, pp. 3−17.

Wagner, W. and Pruss, A., The IAPWS formulation 1995 for the thermodynamic properties of ordinary water substance for general and scientific use, *J. Phys. Chem. Ref. Data*, 2002, vol. 31, no. 2, pp. 387−535.

Zheng, Y.-J., Durben, D.J., Wolf, G.H., and Angell, C.A., Liquids at large negative pressures; water at the homogeneous nucleation limit, *Science*, 1991, vol. 254, pp. 829−832.

Translated by A. Girnis